**HEFAT2014**
**10th International Conference on Heat Transfer, Fluid Mechanics and Thermodynamics**
**14 – 16 July 2014**
**Orlando, Florida**

# NUMERICAL ANALYSIS OF ROTATING RAMPS IN A SCRAMJET ENGINE

Liang J. *, Wei H., Zhen L. and Jun L.
Science and Technology on Scramjet Laboratory
College of Aerospace Science and Engineering,
National University of Defense Technology
Changsha, Hunan 410073
P. R. China
E-mail: jl.snowblwblade@gmail.com

## ABSTRACT

A concept of mixing enhancement forced by rotating ramps has been presented, which based on the design of stationary ramps and Rim-Rotor Rotary Ramjet Engine. The rotating ramps could generate large scale vortex and rotary moving shock waves, which may increase the fuel mixing rate and spread distance in transverse-direction. The commercial software Fluent has been conducted to study the effect of different velocity of ramps rotating on flowfield characteristics. The results show that rotating ramps increase the periodic oscillation of cavity shear layer and induce large streamwise vortices in cavity. When the ramps rotate at a speed of 54.3krpm, the peak value of x-vortex magnitude is nearly four times as the stationary ramps, however, the coefficient of total pressure recovery in the rotating ramps case is nearly 10% less than that in the stationary ramps case. This study provides a new method for mixing enhancement under supersonic airflow condition.

## INTRODUCTION

Supersonic combustion ramjet (scramjet) is a revolutionary engine for airbreathing hypersonic vehicle, the main challenges in the realization of a practical scramjet engine is that fuel mixing and combustion in a short residence time environment is difficult[1]. It is an important issue to keep the combustor length short to reduce the skin friction drag and structure weight, but the rapid fuel/air mixing suffers from low mixing rates due to the stabilizing influence of compressibility on the turbulent mixing layer at high convective Mach numbers. The fuel and air must mix on a large scale then molecular collision is needed which leads to the overall heat release and combustion.

There are a variety of mixing augmentation devices available as outlined by Drummond[2] and Pratt[3] and Seiner[4], most of the mixing augmentation devices are fixed, such as ramps, struts and cavities. Ramps could generate streamwise vortices to enhance mixing, and numerous ramps configurations have been investigated including swept physical ramps, cantileverd ramps, aerodynamic ramps. Another efficient mixing augmentation and flame holder device is cavity. The cavity offers a relatively long residence time for mixing and chemical reactions to take place in the subsonic recirculation. Nevertheless, the wall injection and cavity are insufficient to achieve proper mixing in the flowpath[5].

A W-shaped cowl[6] and a zigzag[7] cavity have been investigated by Kang, the results indicate that the W-shaped cowl could generate pressure fluctuations in the transverse direction and resulted in improved mixing, and the zigzag cavity could generate a transverse directional flow and the combustion induced pressure is 17% higher than the case with the plain cavity, which suggest that the transverse flow may increase the mixing and combustion efficiency. The concept of rim-rotor rotary-ramjet engine (R4E) is introduced by Rancourt[8] and Picard[9], the ramjet shapes spin around a center axis at high-angular velocity and this engine has the potential to significantly improve power density.

In this study, a concept of mixing enhancement forced by rotating ramps has been presented. The windward surface of ramps are designed to be inclined to the axis of the combustor chamber, as the airflow impinges on the ramps, the tangent force would drive ramps to spin. The rotating shock waves generated by ramps leading edge would interfere with the fuel injections, and the swirl flow caused by the ramps would be helpful for fuel spreading in the transverse direction. The concept of rotating ramps is shown in Figure 1.

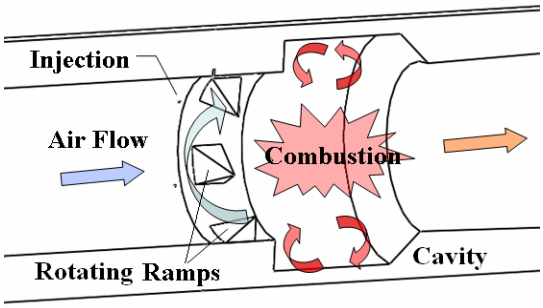


**Figure 1** A concept of rotating ramps

## NUMERICAL MODEL

URANS simulations are performed using the commercial software Fluent that uses an implicit finite volume method. A full second-order discretization of the convective term is used throughout all simulations. Fully turbulent calculations are carried out using the SA turbulence model. Although RANS approaches are not generally as accurate as computational models utilizing Large Eddy Simulation[10] (LES) or Direct Numerical Simulation (DNS) techniques, the computational efficiency afforded by the RANS approach is advantageous and reasonable for the simulation. The convective fluxes are evaluated by Roe flux split scheme, and second order accuracy is obtained with MUSCL schema and a min-mod limiter. The numerical solutions are considered to be converged based on the residual history and the steadiness of the mass flow rate. The calculations are performed using sixteen nodes on the HP BL465c G7 blade system at the Hypersonic Aircraft Research Center.

### Boundary conditions

A fixed uniform inflow is specified at the pressure inlet condition. The supersonic outflow boundary condition is modeled using pressure outlet condition. Adiabatic wall boundary condition is used for the surface of the combustor. Dynamic mesh is used to simulate the rotating motion, and the interface between the rotating zone and stationary zone is modeled using a sliding-mesh approach.

### Validation case

NASA roter 67 is analyzed to validate the numerical model used in present study. NASA rotor 67 is the first stage rotor of a two stage fan, with a design pressure ratio of 1.629 at a mass flow of 33.25 kg/s. The rotor has 22 blades. At the design rotational speed of 16043 rpm the tip relative Mach number is 1.38. The schematic of NASA rotor 67 is shown in Figure 2.

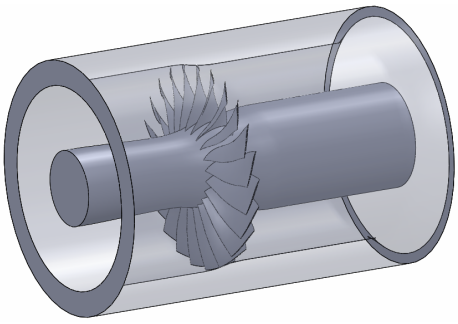

**Figure 2** Schematic of NASA rotor 67

The computed total pressure ratio and adiabatic efficiency at 100 percent speed are plotted against normalized mass flow and compared with experimental data[11] and reference data[12] in Figure 3. The computed total pressure ratio is about 5% less than experimental data, but agrees well with reference data, which is due to the numerical limitation in simulating turbulence boundary layer, vortex, and secondary flows. The computed adiabatic efficiency agrees reasonably well with experimental data.

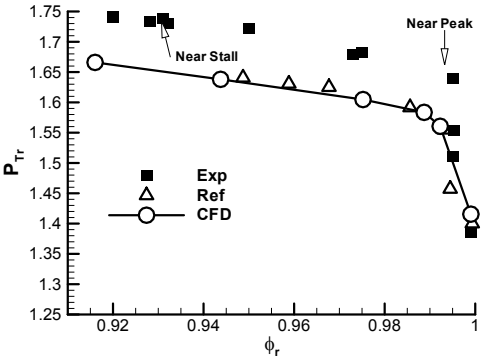


a)

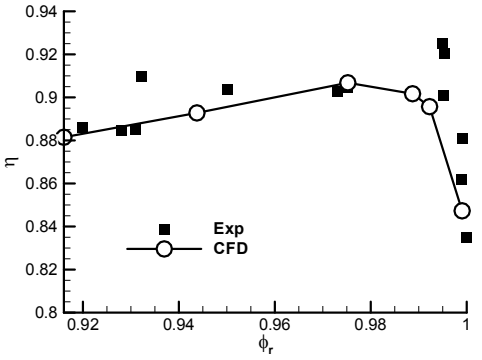


b)

**Figure 3** Performance of NASA rotor 67: a) total pressure ratio as a function of mass flow coefficient, b) adiabatic efficiency as a function of mass flow coefficient

## ROTATING RAMPS INVESTIGATION

In order to evaluate the effect of rotation on the characteristic of combustor flowfield, numerical simulations of ramps rotating at speed of 6krpm and 54.3krpm have been conducted. The combustor illustrated in Figure 4 consists of four parts: isolator, rotating ramps, cavity and expand duct. The overall length of the scramjet flowpath is 1500mm. The isolator has a circular cross-section with a radius of 130mm. The cavity flameholder has a length of 250mm and a depth of 50mm. The cavity is recessed from the surface with a 90-deg rearward-facing step, and spans the entire flowpath width. The trailing edge of the cavity is configured with a 45º ramp. Six ramps with a length of 50mm are placed 35mm upstream of the cavity step.

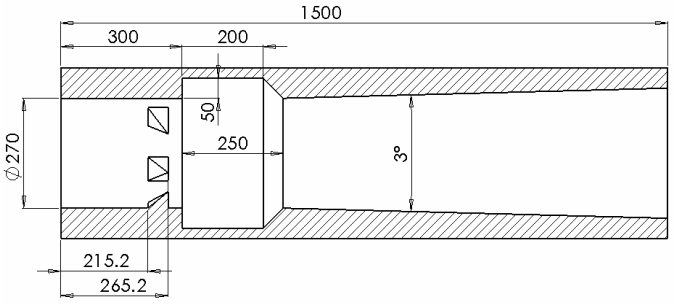


**Figure 4** Schematic of rotating ramps combustor

A structured grid of 1.6×106 nodes is generated around the geometry. The body-fitted grids are clustered towards the walls and around the injector to capture the proper flow physics. The

minimum grid point distance from the surfaces is $1e^{-4}$m. The computational grid is presented in Figure 5.

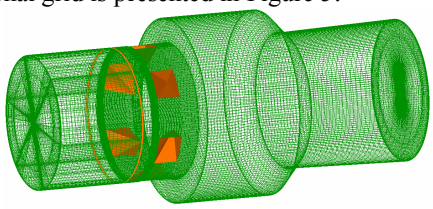

**Figure 5** Computational grid

For the unsteady calculation, the area surrounding the ramps is designated as sliding mesh. Sliding interfaces separate the rotating zone from the stationary zone (Figure 6) which accounts for the interaction between the rotating ramps and the stationary walls. In the rotating zone, the surfaces of ramps are set stationary walls relative to adjacent cell zone. While in the stationary zones, the surfaces of walls are set moving walls with absolute speed of zero.

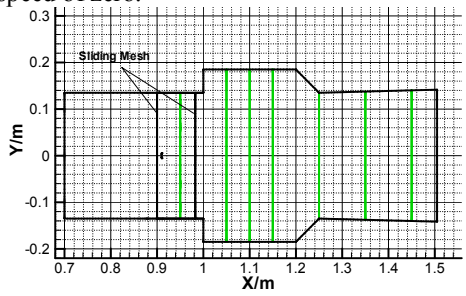


**Figure 6** Position of sliding interfaces

At inlet of the domain, the uniform velocity profile is applied. The inlet total pressure is 1.65MPa, the static pressure is 76.3kPa, and the total temperature is 1483K. At the domain outlet, the static pressure is 76.3kPa, and the total temperature is 300K. Adiabatic wall boundary condition is used for the surface of the combustor.

## RESULTS AND DISCUSSION

Figure 7 shows the initial position of symmetry plane at t=0ms and the phase angle of ramp Φ is zero. A steady-state flowfield is achieved as the ramps are stationary, the characteristics of the flowfield is shown in Figure 8. As the air flow pass through the ramps, the leading edge shock is generated and the streamlines are pushed up to the combustor center. The recirculation zone behind the ramps is merged with that in the cavity. As the air flow pass through the space between ramps, the shear layer flows closely to the surface of wall, which forming a star-like mixing layer structure at the cross section (x=1.05m) near the cavity.

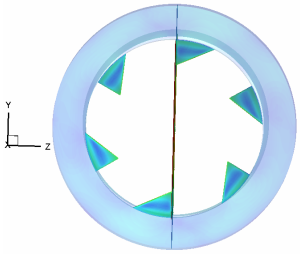

**Figure 7** Initial position of symmetry plane at t=0ms, Φ=0°

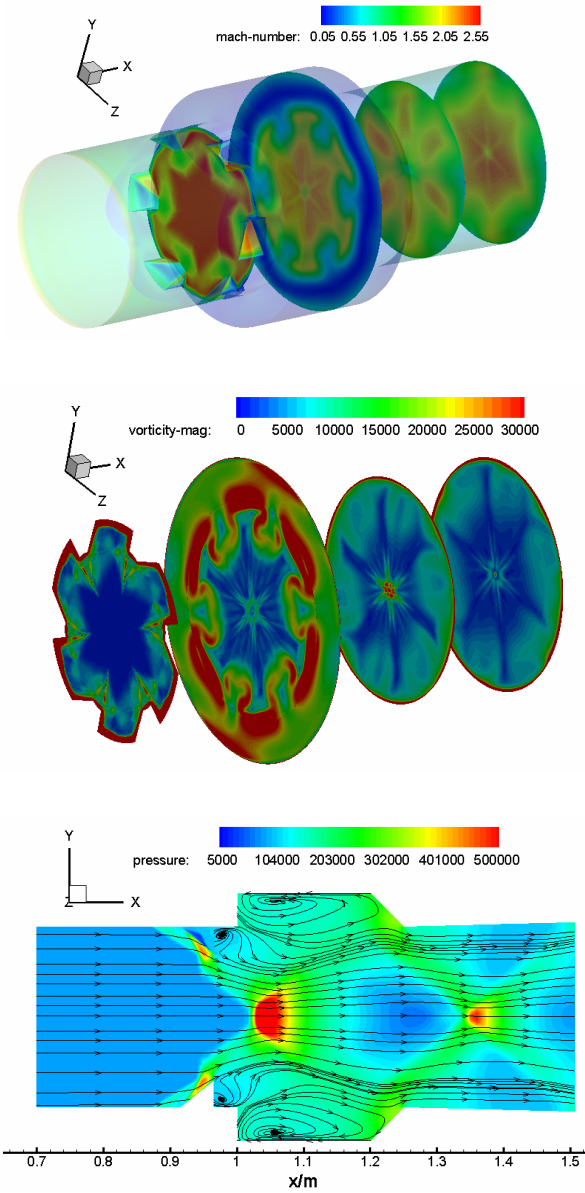


**Figure 8** Flow characteristic of stationary ramps: a) Mach contour, b) vorticity magnitude and c) streamlines and pressure contour

Figure 9 shows the flowfield characteristics in the symmetry plane and cross section as ramps rotating at a speed of 6krpm. At the time t=0.972ms, the phase angle of ramp Φ is about 35 degree, and the shear layer flows closely to the wall, the subsonic zone lies mainly in the cavity. At the time t=1.722ms, the phase angle of ramp Φ is about 62 degree, the subsonic zone behind the ramps expand the region of subsonic zone in the cavity, which forms a blended shear layer. As the ramps rotate, the shear layer of cavity forms a periodic oscillation. This oscillation could destabilize the influence of compressibility on the turbulent mixing layer, and enlarge the region influenced by Kelvin-Helmholtz vortices.

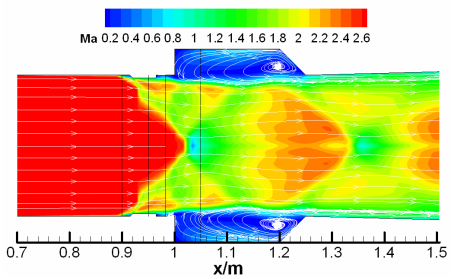


a)

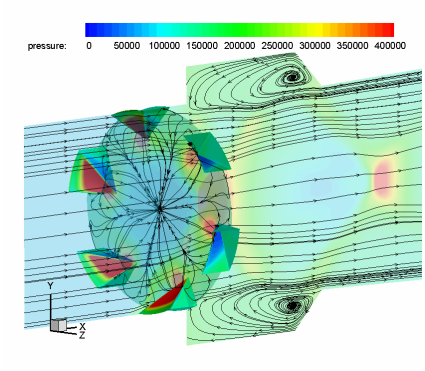


b)

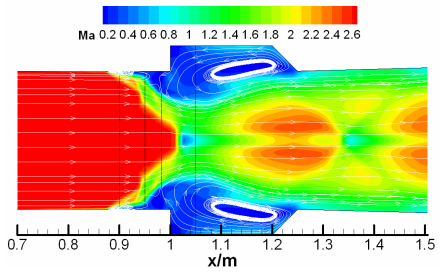


c)

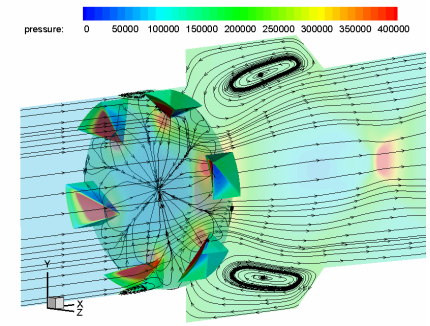


d)

**Figure 9** Flow characteristic of ramps rotating at 6krpm: a) Mach number contours, t=0.972ms，Φ=35°; b) pressure contours and streamlines, t=0.972ms，Φ=35°; c) Mach number contours, t=1.722ms，Φ=62°; d) pressure contours and streamlines, t=1.722ms，Φ=62°

The flowfield characteristic is a little different when the ramp rotating at a speed of 54.3krpm, as is shown in Figure 10. At the time t=0.09ms, the phase angle of ramp Φ is about 29.3 degree, a larger bubble is found in the cavity. At the time t=0.18ms, the phase angle of ramp Φ is about 57.9 degree, the shock wave oscillations alter the flow pattern in the cavity, and three recirculation zones are formed in the cavity which may help fuel mixing and flame anchoring.

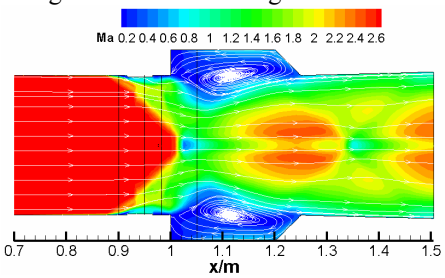


a)

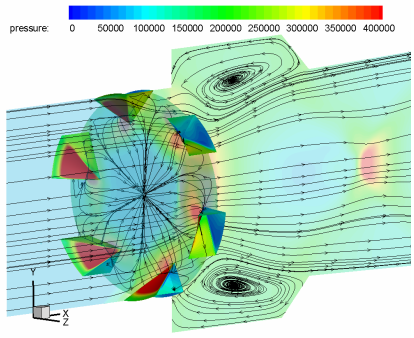


b)

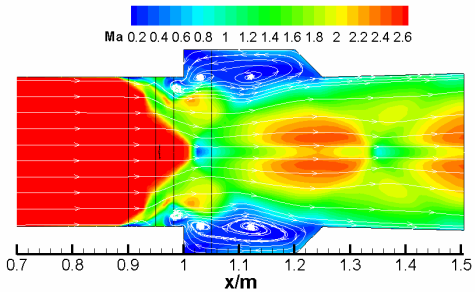


c)

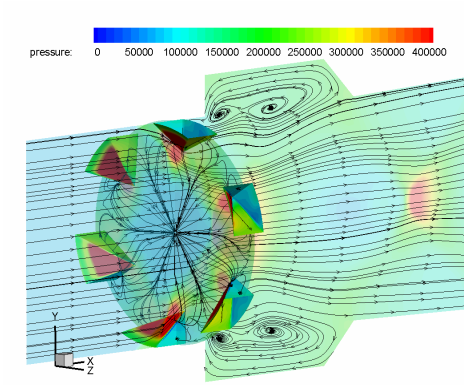


d)

**Figure 10** Flow characteristic of ramps rotating at 54.3krpm: a) Mach number contours, t=0.09ms，Φ=29.3°; b) pressure contours and streamlines, t=0.09ms，Φ=29.3°; c) Mach number contours, t=0.18ms，Φ=57.9°; d) pressure contours and streamlines, t=0.18ms，Φ=57.9°

A reference velocity of 1320m/s and a reference length of 0.8m are used to normalize the cross section averaged x-vortex magnitude, as shown in Figure 11. The differences between the ramps rotating velocity 6krpm case and 0 rpm case are small, while ramps rotating at a velocity of 54.3krpm results in a much higher x-vortex magnitude, with peaks at the position of ramps (x=0.95m) about four times as high as that in the stationary ramps flow. The reason is that the axis of ramps rotating is along the stream, and the positive x-vortex magnitude increases with the rotating velocity. These solutions indicate that the velocity of ramps rotating has a great influence on the x-vortex magnitude.

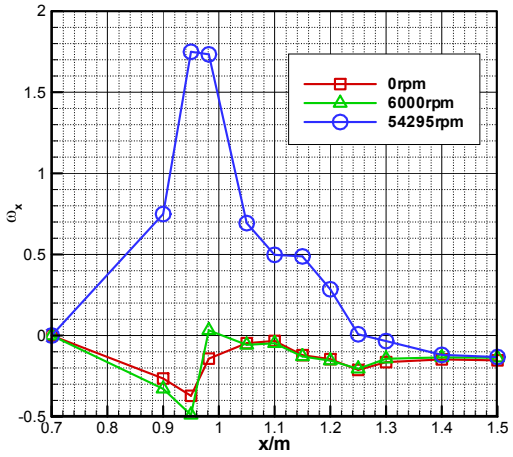


**Figure 11** Distribution of x-vortex magnitude

In order to investigate the flow characteristics of the cross section of ramps, Figure 12 shows the x-vortex magnitude contours and streamlines distribution at x=0.95m plane when ramps rotate at different velocities. Since the ramps rotate at a counterclockwise direction, the streamwise vortex lies mainly in the region behind the perpendicular side of the ramps. When the velocity of ramps increase, more streamlines are forced to move counterclockwise near the wall, and the separate points where streamlines converge move counterclockwise too.

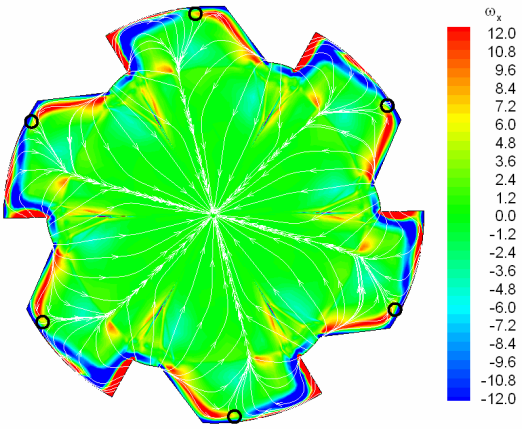

a)

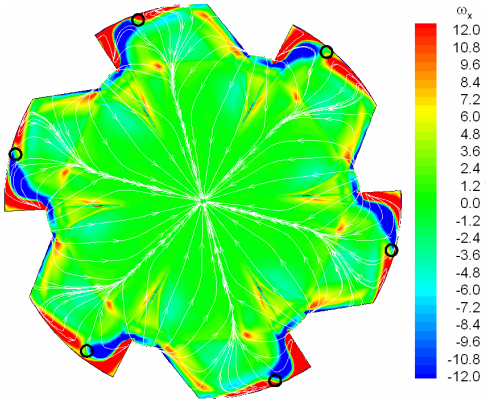

b)

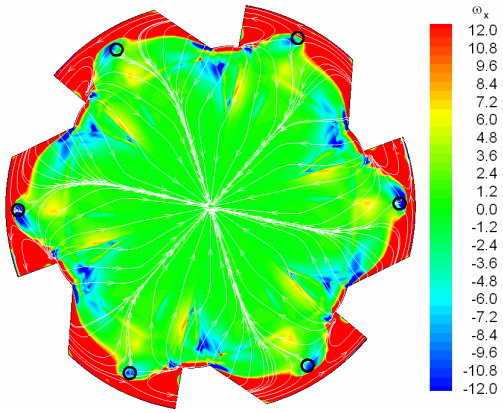

c)

**Figure 12** X-vortex magnitude contours and streamlines distribution at x=0.95m plane when ramps rotate at a velocity of a) 0rpm, b) 6krpm and c) 54.3krpm

Figure 13 shows mass-averaged total pressure recovery coefficients in the cross sections along the combustor axis. The differences between the ramps rotating velocity 6krpm case and 0 rpm case are little, while the total pressure recovery in the 54.3krpm case is about 10% less than the 0 rpm case. The results suggest that the pressure loss in the combustor is mainly caused by the ramps shock, and the pressure loss caused by the rotating flow is little.

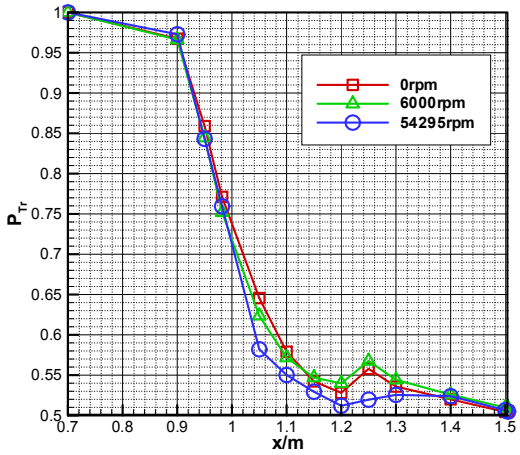


**Figure 13** Distribution of total pressure recovery coefficient

## CONCLUSION

A concept of rotating ramps has been presented for mixing enhancement in turbulent high speed flows. The computational results show that the rotating ramps increase the periodic oscillation of cavity shear layer and induce large streamwise vortices in cavity. When the ramps rotate at a speed of 54.3krpm, the peak value of x-vortex magnitude is nearly four times as the non-rotate ramps, however, the coefficient of total pressure recovery in the rotating ramps case is nearly 10% little than that in the fixed ramps case. This study provides a new method for mixing enhancement under supersonic airflow condition.

## REFERENCES


1) Bushnell, D.M., Hypervelocity Scramjet Mixing Enhancement. *Journal of Propulsion and Power*, 1995. 11(5): pp. 1088–1090.
2) Drummond, J.P. and Carpenter, M.H., Mixing and Mixing Enhancement in Supersonic Reacting Flow-fields. *High-Speed Flight Propulsion Systems, AIAA Progress in Astronautics and Aeronautics*, 1991. 137: pp. 383-455.
3) Pratt, D.T. and Heiser, W.H., *Hypersonic Air-Breathing Propulsion*. AIAA Education Series. 1994.
4) Seiner, J.M., Dash, S.M. and Kenzakowski, D.C., Historical Survey on Enhanced Mixing in Scramjet Engines. *Journal of Propulsion and Power*, 2001. 17(6): pp. 1273–1286.
5) Ben-Yaker, A. and Hanson, R.K., Cavity Flameholders for Ignition and Flame Stabilization in Scramjets: Review and Experimental Study. *AIAA 1998-3122*, 1998.
6) Kang, S.H., Lee, Y.J., Yang, S.S., et al., Cowl and Cavity Effects on Mixing and Combustionin Scramjet Engines. *Journal of Propulsion and Power*, 2011. 27(6): pp. 1169-1177.
7) Kang, S.H., Lee, Y.J. and Yang, S.S., Effects of Flameholder Configurations on Combustion in Scramjet Engines. *Journal of Propulsion and Power*, 2012. 28(4): pp. 739-746.
8) Rancourt, D., Picard, M., Denninger, M., et al., Rim-Rotor Rotary Ramjet Engine, Part 1: StructuralDesign and Experimental Validation. *Journal of Propulsion and Power*, 2012. 28(6): pp. 1293-1303.
9) Picard, M., Rancourt, D., Plante, J.-S., et al., Rim-Rotor Rotary Ramjet Engine, Part 2: Quasi-One-Dimensional Aerothermodynamic Design. *Journal of Propulsion and Power*, 2012. 28(6): pp. 1304-1314.
10) Georgiadis, N.J., Rizzettay, D.P. and Furebyz, C. Large-Eddy Simulation: Current Capabilities, Recommended Practices, and Future Research. AIAA 2009-948. 2009.
11) Chen, J.P., Unsteady Three Dimensional Thin-Layer Navire-Stocks Solutions for Turbomachinery in Transonic Flow. PHD. Mississippi State University, 1991.
12) Wei, L. and GE, N., Numerical Simulation and Test Verification of 3-Dimensional Transonic Navier Stokes Equations Applied to Turbomachinery Rotor Internal Flow. *Journal of Aerospace Power*, 2005. 20(2): pp. 262-266.